

In light of the spectra discussed below for the shorter chain compounds it is likely that exchange interactions also play a significant role in the line broadening observed for the adducts of III and IV.

The spectra of the six-coordinate adducts of I and II bear no resemblance to normal frozen-solution nitroxyl EPR spectra. The nitroxyl lines are severely broadened and spread over several hundred Gauss. For I-bipy the low-field and high-field turning points are at 2600 and 3400 G, respectively (Figure 4A). The spectrum of I-(py)₂ is slightly more spread out (turning points at 2400 and 3600 G, respectively). Even for II (*n* = 1) the low-field and high-field turning points in the spectrum of II-(py)₂ are at 2900 and 3600 G, respectively. The spectra of the six-coordinate adducts of I and II do not saturate at the highest microwave powers available on our spectrometer. These observations indicate significant mixing of the nickel and nitroxyl wave functions.³³ CPK molecular models indicate that the interspin distances are about 7 and 8 Å respectively for the nitrogenous base adducts of I and II. The observed splittings in the spectra are too large to be explained by purely dipolar interaction at these distances. Thus it appears that a substantial exchange interaction must be invoked to explain the large shifts in the spectra.

The observation of large splittings in the frozen-solution spectra is noteworthy in another respect. We expect that when a nitroxyl interacts with a rapidly relaxing metal the appearance of the nitroxyl portion of the spin-coupled spectrum will be dependent on the rate of the metal relaxation compared with the splittings in the spectrum. When the metal relaxation rate is comparable to the splittings in the nitroxyl lines, a broadened spectrum is expected. When the metal relaxation rate is fast relative to the potential splittings of the nitroxyl lines, the splittings will be averaged out. In between these two limits, the widths of the nitroxyl lines should be a function of the metal relaxation rate

(33) Throughout the text the observed EPR lines are referred to as nitroxyl lines which is the assignment of the transitions in the limit as *J* approaches 0.

and of the spin-spin interaction. These arguments are analogous to those used in the analysis of temperature-dependent EPR and NMR spectra of dynamic systems. Since information is not available concerning the nickel relaxation rates in these compounds and since the transitions have not been assigned, it is not possible to determine the extent to which the line shapes and line positions reflect the partial collapse of larger splitting due to a nickel relaxation rate which is not sufficiently rapid to completely average out the spin-spin interaction. Further studies are needed to estimate the metal relaxation times, zero field splittings, and exchange interactions in these molecules.

Conclusions

The nickel-nitroxyl interaction in nitrogenous base adducts of I-V decreases rapidly as *n* increases. However, even in V the spin-spin interaction is detectable. In fluid solution the flexible hydrocarbon chains in the compounds with *n* = 2, 4, or 6 permit intramolecular nickel-nitroxyl interactions which are strongly dependent on the solution viscosity. The large splittings in the frozen solution spectra of the six-coordinate adducts of I and II indicate that exchange makes a significant contribution to the spin-spin interaction.

Acknowledgment. This work was supported in part by NIH grant GM21156 and the donors of the Petroleum Research Foundation, administered by the American Chemical Society. We are grateful to Prof. Kosman (SUNY Buffalo) for providing us with unpublished details of the syntheses reported in ref 20 and to Prof. Hornback and Dr. More for helpful discussions concerning the syntheses.

Registry No. I, 85361-86-0; II, 85361-88-2; III, 88945-48-6; IV, 88945-49-7; V, 88945-50-0; VI, 88932-76-7; VII, 88932-77-8; VIII, 31146-15-3; IX, 88932-78-9; X, 88932-79-0; XI, 88932-80-3; XII, 88932-81-4; XIII, 88932-82-5; XIV, 88932-83-6; XV, 88932-84-7; XVI, 88932-85-8; XVII, 88932-86-9; XVIII, 88932-87-0; tempone, 2896-70-0; triethyl phosphonoacetate, 867-13-0; triethyl 4-phosphonocrotonate, 10236-14-3.

Redox Conduction in Single and Bilayer Films of Redox Polymer

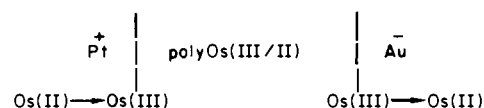
P. G. Pickup,[†] W. Kutner,[†] C. R. Leidner, and Royce W. Murray*

Contribution from Kenan Laboratories of Chemistry, University of North Carolina, Chapel Hill, North Carolina 27514. Received August 8, 1983

Abstract: Polymeric films made from Ru and Os polypyridine complexes and sandwiched between potential-controlled Pt and porous Au electrodes exhibit low resistance to current flow when the electrode potentials are such as to generate mixed-valent states in the polymers, and high resistances when the films are composed of only one oxidation state. The observed current-potential curves with their limiting currents can be understood in terms of a concentration gradient (not potential gradient) driven flow of electrons with effective mobility characterized by an electron diffusion coefficient *D*_{ct}. Sandwich-electrode measurements of *D*_{ct} for the M(III/II) mixed-valent state agree with those produced by other methods, and estimates from *D*_{ct} of effective electron self-exchange rates in the polymers come close to those known for homogeneous solution self-exchange rates between [M(bpy)₃]ⁿ⁺ complexes. For poly[Os(bpy)₂(vpy)₂]²⁺ films, the electron mobility varies in the proportion 1:3:25 for the three mixed-valent states Os(III/II), Os(II/I), and Os(I/0), respectively. The most highly conducting state can pass currents of 0.6 A/cm².

Our¹ and others^{2,3} interest in electron transport in thin films of electroactive polymers stems from fundamental questions about electron mobility in these materials and from its connection to potential applications of the films to electrocatalysis,^{21,4} photo-

Scheme 1



[†] Permanent address: Institute of Physical Chemistry, Polish Academy of Sciences, Kasprzaka 44,01-224 Warsaw, Poland.

* Department of Chemistry, State University of New York at Buffalo.

electrochemistry,⁵ and chemical devices.^{1h} When studied by transient methods,^{1a,2b} the electron transport follows diffusion laws

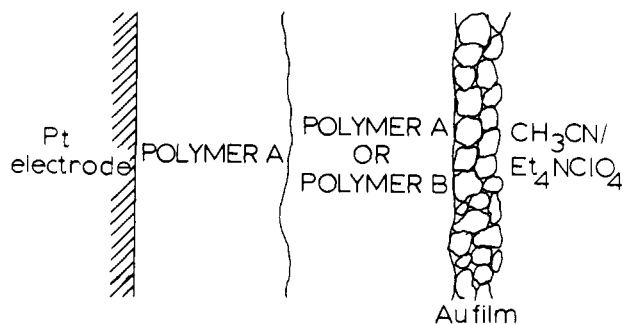


Figure 1. Schematic sandwich electrode.

and can be characterized by a diffusion coefficient D_{ct} . Electron transport is thought^{2e} in most of these materials to occur by electron self-exchange between neighbor oxidized and reduced redox sites in the polymer, which is peculiar to the mixed-valent state of the polymer. Physical diffusion of the redox sites also effects electron transport, combining its rate with that of electron self-exchange.^{1n,3a,j,k} especially when the redox site is an ion electrostatically trapped³ in an ion-exchange polymer. When the redox site is affixed to the polymer framework, its physical diffusion is more restricted, but microscopically can still be important.^{lj} This report deals with polymers with affixed redox sites (redox polymer); we refer to the electron self-exchange-driven currents in these polymers as "redox conduction currents".

We recently described^{1h} how to measure steady-state redox conduction currents in ultrathin redox polymer films wetted with a solvent containing a supporting electrolyte. The polymer film is sandwiched between two metal electrodes, one of which is porous and contacted by the solvent. This paper describes "sandwich-

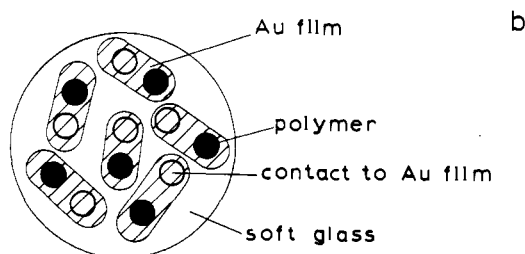
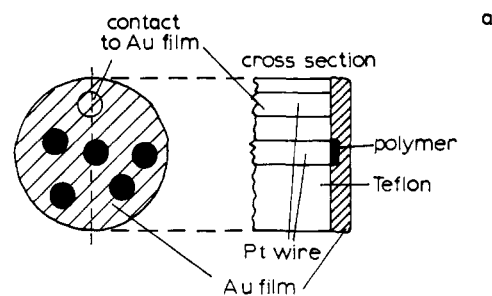


Figure 2. Schematic representation of multi-mini-sandwich electrode assembly embedded in Teflon (a) and glass (b).

electrode" measurements of D_{ct} for the M(III/II) mixed-valent states of three related osmium and ruthenium complex polymer films, of two highly reduced mixed-valent oxidation states of one of the polymers, and of an overlaid film of two different polymers (a bilayer⁶). No previous electron mobility data exist for highly reduced, electrolyte, and solvent-swollen redox polymers, in part because of the poor stability of such states.⁷ Nor has the electron mobility in a series of mixed-valent states of the same redox polymer been compared, although results have been recently reported^{3a} for redox ions electrostatically trapped in Nafion films. D_{ct} measured as a function of mixed-valent state has use in assessing the relative importance of polymer lattice and counterion mobilities and intrinsic electron self-exchange rate in electron mobility.

The sandwich electrode (Figure 1) consists of a ca. 100–1000-nm polymer film (or bilayer of polymer films) reductively electropolymerized^{ld,8} onto a Pt disk electrode, with a porous gold film electrode (ca. 50–100 nm) vapor deposited over the polymer. The gold electrode porosity allows entry of solvent and supporting electrolyte ions into the polymer film. Charge-compensating counterions can then migrate in/out of the polyionic film as its oxidation state is changed, so that the polymer remains fully electroactive. Three of the sandwich electrodes described use films of a single polymer, i.e., Pt/poly[Os(bpy)₂(vpy)₂]²⁺/Au, Pt/poly[Ru(bpy)₂(vpy)₂]²⁺/Au, and Pt/poly[Ru(vbpy)₃]²⁺/Au, and one has overlaid films of two different polymers (a bilayer⁶), i.e., Pt/poly[Ru(bpy)₂(vpy)₂]²⁺/poly[Os(bpy)₂(vpy)₂]²⁺/Au, where bpy = 2,2'-bipyridine, vbpy = 4-methyl-4'-vinyl-2,2'-bipyridine, and vpy = 4-vinylpyridine. We cause one electrode to act as an electron sink and the other as an electron source, by applying potentials to them so as to oxidize and reduce, respectively, the polymer redox sites contacting the electrodes. Steady-state currents flow at both electrodes, since steady-state concentration gradients of oxidized and reduced sites are generated across the film. At applied electrode potentials which do not generate redox

(1) (a) Daum, P.; Lenhard, J. R.; Rolison, D. R.; Murray, R. W. *J. Am. Chem. Soc.* **1980**, *102*, 4649. (b) Nowak, R. J.; Schultz, F. A.; Umana, M.; Lam, R.; Murray, R. W. *Anal. Chem.* **1980**, *52*, 315. (c) Daum, P.; Murray, R. W. *J. Phys. Chem.* **1981**, *85*, 389. (d) Denisevich, P.; Abruna, H. D.; Leidner, C. R.; Meyer, T. J.; Murray, R. W. *Inorg. Chem.* **1982**, *21*, 2153. (e) Ikeda, T.; Leidner, C. R.; Murray, R. W. *J. Electroanal. Chem.* **1982**, *138*, 343. (f) Burgmayer, P.; Murray, R. W. *Ibid.* **1982**, *135*, 335. (g) Schmehl, R. H.; Murray, R. W. *Ibid.* **1983**, *152*, 97. (h) Pickup, P.; Murray, R. W. *J. Am. Chem. Soc.* **1984**, *105*, 4510. (i) Denisevich, P.; Willman, K. W.; Murray, R. W. *Ibid.* **1981**, *103*, 4727. (j) Facci, J. S.; Schmehl, R. H.; Murray, R. W. *Ibid.* **1982**, *104*, 4959. (k) Nakahama, S.; Murray, R. W. *J. Electroanal. Chem.* **1983**, *158*, 303. (l) Kuo, K. N.; Murray, R. W. *Ibid.*, **1982**, *131*, 37. (m) Facci, J.; Murray, R. W. *Ibid.*, **1982**, *124*, 339. (n) Facci, J.; Murray, R. W. *J. Phys. Chem.* **1981**, *85*, 2870.

(2) (a) Peerce, P. J.; Bard, A. J. *J. Electroanal. Chem.* **1980**, *114*, 89. (b) Oyama, N.; Anson, F. C. *J. Electrochem. Soc.* **1980**, *127*, 640. (c) Chambers, J. Q. *J. Electroanal. Chem.* **1981**, *130*, 381. (d) Schroeder, A. H.; Kaufman, F. B.; Patel, V.; Engler, E. M. *Ibid.*, **1980**, *113*, 193. (e) Kaufman, F. B.; Schroeder, A. H.; Engler, E. M.; Kramer, S. R.; Chambers, J. Q. *J. Am. Chem. Soc.* **1980**, *102*, 483. (f) Kaufman, F. B.; Engler, E. M. *Ibid.*, **1979**, *101*, 547. (g) Thompson, W. A.; Schroeder, A. H.; Kaufman, F. B. *J. Vac. Sci. Technol.* **1981**, *18*, 243. (h) Shigehara, K.; Oyama, N.; Anson, F. C. *J. Am. Chem. Soc.* **1981**, *103*, 2552. (i) Anson, F. C. *J. Phys. Chem.* **1980**, *84*, 3336. (j) Andrieux, C. P.; Saveant, J.-M. *J. Electroanal. Chem.* **1980**, *111*, 377. (k) Laviron, E. *Ibid.* **1980**, *112*, 1. (l) Laviron, E.; Roullier, L.; DeGrand, C. *Ibid.* **1980**, *112*, 11. (m) Fukui, M.; DeGrand, C.; Miller, L. L. *J. Am. Chem. Soc.* **1982**, *104*, 28. (n) DeGrand, C.; Miller, L. L. *J. Electroanal. Chem.* **1982**, *132*, 163. (o) Albergy, W. J.; Boutelle, M. G.; Colby, P. J.; Hillman, A. R. *Ibid.* **1982**, *133*, 135. (p) Bookbinder, D. C.; Wrighton, M. S. *J. Electrochem. Soc.*, in press.

(3) Anson, F. C.; Buttry, D. A. *J. Am. Chem. Soc.* **1983**, *105*, 658. (b) Oyama, N.; Anson, F. C. *J. Electrochem. Soc.* **1980**, *127*, 247. (c) Buttry, D. A.; Anson, F. C. *J. Am. Chem. Soc.* **1982**, *104*, 4824. (d) Oyama, N.; Yamaguchi, S.; Nishiki, Y.; Tokuda, K.; Matsuda, H.; Anson, F. C. *J. Electroanal. Chem.* **1982**, *139*, 371. (e) Anson, F. C.; Saveant, J.-M.; Shigehara, K. *J. Am. Chem. Soc.* **1984**, *105*, 1096. (f) Ohsaka, T.; Anson, F. C. *J. Phys. Chem.* **1983**, *87*, 640–647. (g) Rubinstein, I.; Bard, A. J. *J. Am. Chem. Soc.* **1980**, *102*, 6641. (h) Rubinstein, I.; Bard, A. J. *Anal. Chem.* **1981**, *53*, 102. (i) Henning, T. P.; White, H. S.; Bard, A. J. *J. Am. Chem. Soc.* **1981**, *103*, 3937. (j) White, H. S.; Leddy, J.; Bard, A. J. *Ibid.* **1982**, *104*, 4811. (k) Martin, C. R.; Rubinstein, I.; Bard, A. J. *Ibid.* **1982**, *104*, 4817. (l) Faulkner, L. R.; Majda, M. *J. Electroanal. Chem.* **1982**, *137*, 149. (m) Faulkner, L. R.; Shaw, B. R.; Haight, G. P., Jr. *Ibid.* **1982**, *140*, 147.

(4) (a) Andrieux, C. P.; Dumas-Bouchiat, J. M.; Saveant, J.-M. *J. Electroanal. Chem.* **1982**, *131*, 1. (b) Murray, R. W. *Phil. Trans. R. Soc. London, Ser. A* **1981**, *302*, 253.

(5) Wrighton, M. S., *ACS Symp. Ser.* **1982**, No. 192, 99.

(6) Denisevich, P.; William, K. W.; Murray, R. W. *J. Am. Chem. Soc.* **1981**, *103*, 4727.

(7) Kerr, J. B.; Miller, L. L.; Van De Mark, M. R. *J. Am. Chem. Soc.* **1980**, *102*, 3383.

(8) (a) Abruna, H. D.; Denisevich, P.; Umana, M.; Meyer, T. J.; Murray, R. W. *J. Am. Chem. Soc.* **1981**, *103*, 1. (b) Calvert, J. M.; Schmehl, R. H.; Sullivan, B. P.; Facci, J. S.; Meyer, T. J.; Murray, R. W. *Inorg. Chem.* **1983**, *22*, 2151.

site concentration gradients, the films are insulators in the sense that there are no redox conduction currents. It can be seen that electron mobility and the flow of redox conduction currents in these sandwich cells is determined by quite different considerations from those in conductivity measurements on dry films,⁹ where electron flow is driven by voltage, not concentration gradients.

Experimental Section

Potential Control. Of the several experimental ways¹⁰ to apply potentials to the two electrodes of the sandwich, the most versatile uses a four-electrode potentiostat (bipotentiostat) which independently controls their potentials relative to a reference electrode placed in the electrolyte/solvent part of the cell.¹¹ The difference between the two potentials can be small or large; one can be fixed and the other scanned with time (both relative to the reference electrode), or both potentials scanned with a fixed difference between them. Most experiments here scan the Pt electrode potential (E_{Pt}) while the potential of the gold electrode (E_{Au}) is kept constant. The current at each of the two working electrodes and therefore the current flowing through the polymer is measured as a function of the potentials of the two electrodes.

Electrodes. A second-generation sandwich electrode was employed, based on a multi-mini-electrode assembly composed of the polished ends of six fine Pt wires (diameter 0.064 cm, $A = 0.0032 \text{ cm}^2$) embedded in a Teflon shroud (Figure 2a). This allowed five sandwich electrodes to be constructed simultaneously (the sixth electrode was not coated with polymer and served as a contact to the gold film), an important advantage considering that only ca. 50% of the sandwiches (compared to 10% in earlier experiments^{1b}) yielded any results (see below). An improved, glass-shrouded version of the electrode (Figure 2b) was used for the Os(II/I), Os(I/0), and variable-temperature parts of the study. The electrode was masked during Au deposition so as to form the indicated six polymer-coated electrode-connecting electrode pairs of Pt wire tips. [The glass shroud made it easier to maintain the Pt microdisk and surrounding shroud surface in the same plane during polishing. The polishing was done on a diamond (1 μm , Buehler) paste-coated paper card resting on a hard surface.]

Syntheses of the electroactive monomers $[\text{Os}(\text{bpy})_2(\text{vpy})_2]^{2+}$, $[\text{Ru}(\text{bpy})_2(\text{vpy})_2]^{2+}$, and $[\text{Ru}(\text{vbpy})_3]^{2+}$, and their electropolymerization to form films on electrodes are described elsewhere.^{1d,8} To prepare, for example, a Pt/poly $[\text{Os}(\text{bpy})_2(\text{vpy})_2]^{2+}$ /Au sandwich, the Pt disk electrode was coated with a film of the osmium polymer by repeated potential sweeps between -1.0 and -1.7 V vs. SSCE in a ca. 0.5 mM, thoroughly degassed, acetonitrile solution of the monomer complex. After the electrode was washed with acetone and air-dried, gold vapor deposition was performed using a Veeco V-300 depositor, resistively heating the gold to yield deposition rates on the polymer of 0.2 to 5 $\text{\AA}/\text{s}$ at pressures of 2 to 5 $\times 10^{-5}$ torr and gold films of average thickness 50–100 nm. The deposition rate was increased as deposition proceeded. The surface coverages of redox sites ($\Gamma_{T,\text{Os}}$ or $\Gamma_{T,\text{Ru}}$) were determined both before and after (with no significant changes in Γ_T for the electrodes used) gold deposition, by measuring the electrochemical charge under slow potential scan M(III/II) cyclic voltammograms. The values of Γ_T are converted into film thickness using dry-weight polymer density, which corresponds to a redox site concentration in the poly $[\text{Os}(\text{bpy})_2(\text{vpy})_2]^{2+}$ polymer of $1.5 \times 10^{-3} \text{ mol}/\text{cm}^3$ and in the poly $[\text{Ru}(\text{bpy})_2(\text{vpy})_2]^{2+}$ of $1.6 \times 10^{-3} \text{ mol}/\text{cm}^3$.

Electrochemical experiments were in 0.1 M $\text{Et}_4\text{NClO}_4/\text{acetonitrile}$ with conventional cells and equipment. A homemade bipotentiostat similar to that described in the Bard and Faulkner text¹³ and a Model RDE3 bipotentiostat (Pine Instrument Co., Grove City, PA) were used. Electrochemical potentials are referenced to the NaCl-saturated SCE (SSCE).

Electrode Conditioning. As before,^{1b} many sandwich electrodes initially exhibited an electrical short between the Pt electrode and the Au

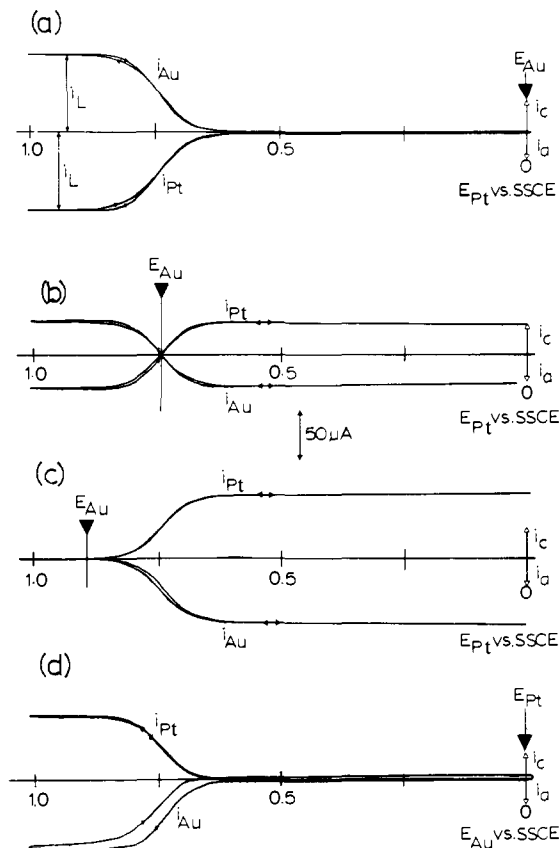


Figure 3. Four-electrode (bipotentiostat) cyclic voltammetry at 20 mV/s of $4.7 \times 10^{-8} \text{ mol}/\text{cm}^2$ ($d = 280 \text{ nm}$) Pt/poly $[\text{Os}(\text{bpy})_2(\text{vpy})_2]^{2+}$ /Au sandwich electrode. Curves a–c: E_{Pt} scanned at 20 mV/s and $E_{Au} = 0, +0.74, +0.9 \text{ V}$ vs. SSCE, respectively. Curve D: $E_{Pt} = 0 \text{ V}$ and E_{Au} scanned at 20 mV/s. Electrode area = 0.0032 cm^2 , 0.1 M $\text{Et}_4\text{NClO}_4/\text{CH}_3\text{CN}$.

film, which could often be broken via oxidizing the shorting gold particles or filaments with a brief potentiostating of the Pt electrode at +1.5 V, i.e., "conditioning". Even so, many electrodes (individual surfaces on a multielectrode assembly) could not be used (failures). This depended strongly on the total surface coverage Γ_T of polymer(s). In the case of the osmium polymer, for $\Gamma_T < 5 \times 10^{-8} \text{ mol}/\text{cm}^2$, 90% were failures. For $5 \times 10^{-8} < \Gamma_T < 1 \times 10^{-7} \text{ mol}/\text{cm}^2$, only 30% were failures. For $\Gamma_T > 1 \times 10^{-7} \text{ mol}/\text{cm}^2$, shorting was still a problem, but often when there was not a short there was poor electrical contact between the Au film and the polymer. Seventy-five percent of the glass-shrouded electrodes gave redox conduction currents when $5 \times 10^{-8} < \Gamma_T < 1.5 \times 10^{-7} \text{ mol}/\text{cm}^2$. When films of poly $[\text{Ru}(\text{bpy})_2(\text{vpy})_2]^{2+}$ or poly $[\text{Ru}(\text{vbpy})_3]^{2+}$ were used, conditioning was not possible because the gold film is oxidized by the Ru(III) states of these polymers. Fortunately, ca. 50% of these electrodes were not initially shorted.

Results and Discussion

Redox Conduction Currents for the M(III/II) Couple in Poly $[\text{Os}(\text{bpy})_2(\text{vpy})_2]^{2+}$, Poly $[\text{Ru}(\text{bpy})_2(\text{vpy})_2]^{2+}$, and Poly $[\text{Ru}(\text{vbpy})_3]^{2+}$ Films. To obtain a typical voltammogram for a Pt/poly $[\text{Os}(\text{bpy})_2(\text{vpy})_2]^{2+}$ /Au sandwich (Figure 3a), E_{Au} was held at 0 V, while E_{Pt} was slowly scanned toward positive potentials past $E^{o'}$ (+0.73 V) for the Os(II→III) reaction of the polymer and back again. The currents at each electrode are shown as a function of E_{Pt} (vs. SSCE). Note that the $E_{1/2}$ for half-maximum current is +0.74 V (very close to $E^{o'}$ for the polymer), and that a limiting current $i_{L} = 75 \mu\text{A}$ (23 mA/cm^2) is observed at sufficiently positive E_{Pt} . Except for a minor hysteresis,¹⁴ the currents at scan rates $\leq 20 \text{ mV}/\text{s}$ are steady state and depend little on the scan direction of the Pt electrode.

We symbolize this experiment with the notation shown in Scheme I. At sufficiently positive potentials the Pt electrode

(14) The currents on the negative- and positive-going potential scans are not exactly the same.

(9) (a) Cowan, D. O.; Park, J.; Pittman, C. U.; Sasaki, Y.; Mukherjee, T.; Diamond, N. A. *J. Am. Chem. Soc.* **1972**, *94*, 5110. (b) Pittman, C. U.; Sasaki, Y.; Mukherjee, T. *Chem. Lett.* **1975**, 383. (c) Pladke, S. D.; Sathianandan, K.; Karekar, R. N. *Thin Solid Films* **1978**, *51*, L9.

(10) In a three-electrode potentiostat, with working and auxiliary connections made to the two sandwich electrodes, the potential of only the working electrode is controlled. With a two-electrode potentiostat, the sandwich-electrode potentials are controlled only with respect to one another. Such experiments are described elsewhere.^{1b}

(11) An auxiliary electrode is also in the electrolyte solution, and a four-electrode potentiostat is used in the manner of twin electrode thin layer electrochemistry.¹²

(12) Anderson, L. B.; Reilley, C. N. *J. Electroanal. Chem.* **1965**, *10*, 295.

(13) Bard, A. J.; Faulkner, L. R. "Electrochemical Methods"; Wiley: New York, 1980.

Table I. Electron Diffusion Coefficients Expressed as $D_{ct}^{1/2}C_T$ for Os(III/II) and Ru(III/II) Mixed-Valent Polymers, by Different Methods

polymer	$D_{ct}^{1/2}C_T \times 10^8, \text{ mol/cm}^2 \text{ s}^{1/2}$		
	sandwich electrode ^a	chronoamperometry ^b	mediation ^c
poly[Os(bpy) ₂ (vpy) ₂] ²⁺	8.5, 7.3, 10.7, 13.2 9.0, 11.0, 16.0, 11.4		10.6 ^e
poly[Os(bpy) ₂ (p-cinn) ₂] ²⁺	av 10.9 ± 2.0 ^d 5.1, 3.4, 3.2, 3.4, 7.2 ^f 3.8, 3.2	4.3 ^g	
poly[Ru(vbpy) ₃] ²⁺	av 4.2 ± 1.1 5.6	2.1, 2.4 ^h av 2.2 ± 0.2	3.3, 4.8, 4.8, 3.2 ⁱ av 4.0 ± 0.8 6.9, 5.0, 4.4, 4.0 ^j av 5.1 ± 0.6
poly[Ru(bpy) ₂ (vpy) ₂] ²⁺	4.7, 5.9, 3.5, 3.1 av 4.3 ± 1.0	3.2 ^k	

^a Using sandwich electrodes as in Figure 2a. ^b Potential step chronoamperometry. ^c M(III) states in the film mediate oxidation of a solution complex or of a second polymer film in a bilayer electrode at a rate limited by D_{ct} . ^d Measurements on electrodes with $\Gamma_T = 1.8, 2.6, 4.7, 6.4, 6.5, 7.3, 7.4, 8.0 \times 10^{-8} \text{ mol/cm}^2$, in order given. ^e Reference 21. ^f Reference 1h. ^g Reference 1j. ^h Reference 1d. ⁱ Reference 1c. ^j Leidner, C. R.; Denisevich, P.; Willman, K.; Murray, R. W. *J. Electroanal. Chem.*, in press. ^k Kuo, K. N. University of North Carolina, unpublished results, 1981.

generates oxidized polymer sites which diffuse by electron exchange with reduced sites to the Au electrode where the Os(III) sites are reduced. The anodic current at the Pt electrode in the voltammogram of Figure 3a is derived^{1h,12} by invoking Fick's first law to represent the linear concentration gradient of Os(III) sites across the film, and by noting that [Os(III)] is 0 at the Au electrode and is given by the Nernst equation at the Pt electrode:

$$i_{Pt} = - \frac{nFAD_{ct}C_T^2}{\Gamma_T(1 + \exp[(gnF/RT)(E^\circ - E])]} \quad (1)$$

where D_{ct} is the electron diffusion coefficient, g is a parameter (vide infra) ideally equal to 1, and Γ_T and C_T are the coverage (mol/cm²) and concentration (mol/cm³), respectively, of electroactive Os sites in the redox polymer. The cathodic current at the Au electrode is the same, but oppositely signed. Equation 1 predicts (i) that the half-limiting current occurs at E° , which is observed, (ii) that limiting current occurs when the polymer is 1:1 Os(III):Os(II) (which is the situation when all redox sites adjacent to the Pt electrode are Os(III), i.e., $E_{Pt} > E^\circ + 120 \text{ mV}$, all redox sites adjacent to the gold film are Os(II), and linear, steady-state concentration gradients of Os(II) and Os(III) exist across the polymer), and (iii) that the limiting current i_L is related to the electron diffusion coefficient (D_{ct}) of the polymer, by

$$i_L = nFAD_{ct}C_T^2/\Gamma_T \quad (2)$$

Equations 1 and 2 are analogous to those of twin electrode thin layer electrochemistry,¹² except that there diffusion is accomplished by physical mass transport of the redox species. Also, eq 1 is formally the same as the so-called Case E of electron-transfer mediated electrocatalysis⁴⁸ where a steady supply of a chemical reductant serves the role of the second electrode.

The extent of polymer swelling is not directly known, and so the parameter we obtain from eq 2, without any assumptions, is $D_{ct}C_T^2$, or to compare with chronoamperometric results, $D_{ct}^{1/2}C_T$. Results for $D_{ct}^{1/2}C_T$ for a series of osmium polymer sandwiches and for the ruthenium polymers are given in Table I. The voltammograms for Pt/poly[Ru(bpy)₂(vpy)₂]²⁺/Au and Pt/poly[Ru(vbpy)₃]²⁺/Au sandwiches are similar to that of Figure 3a, except that $E_{1/2}$ occurs for each at the respective E° of the polymer Ru(III/II) wave, 1.16 and 1.22 V. The value of $D_{ct}^{1/2}C_T$ according to eq 2 should not vary with Γ_T , and although there is some scatter in $D_{ct}^{1/2}C_T$, no significant trend seems present. Also, according to eq 1, $E_{1/2}$ should not vary with Γ_T , and within ca. ±10 mV, it does not. Table I also shows $D_{ct}^{1/2}C_T$ values determined previously by other methods. The agreement between steady-state (sandwich and mediation) and transient (chronoamperometry) measurements is fairly good except for a twofold difference for older results^{1d} for poly[Ru(vbpy)₃]²⁺, where polymer

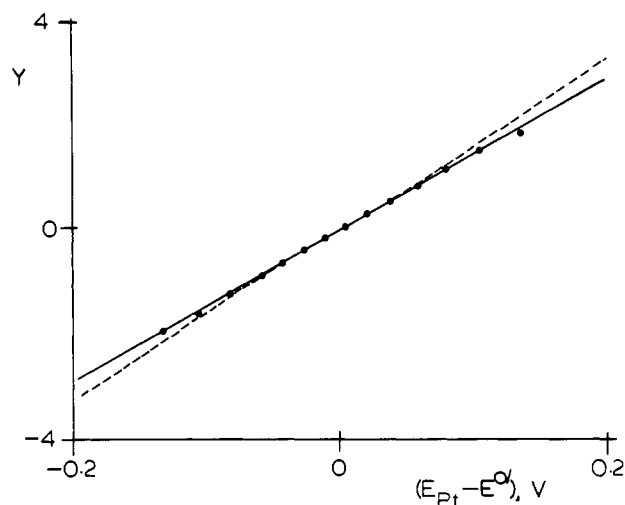


Figure 4. (●) Plot of experimental $\log[i/(i_L - i)]$ vs. $E_{Pt} - E^\circ$ for steady-state redox conduction through a $7.3 \times 10^{-8} \text{ mol/cm}^2$ Pt/poly[Os(bpy)₂(vpy)₂]²⁺/Au sandwich electrode at $E_{Au} = 0 \text{ V}$: (—) plot of eq 4 ($Y = \log [i/(i_L - i)]$) for $g = 0.84$; (---) plot of eq 5 of ref 1e ($Y = \log [f/(1 - f)]$) for $G = -0.67$.

degradation may have been an unrecognized problem.

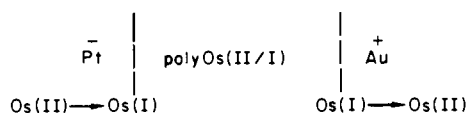
Equation 1 does not, however, for $g = 1$, accurately describe the rising part of the voltammogram of Figure 3a, as shown by combining eq 1 and 2:

$$E = E^\circ + (RT/gnF) \ln [i/(i_L - i)] \quad (3)$$

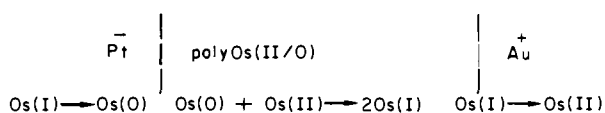
and plotting $\log [i/(i_L - i)]$ vs. E for data collected by pausing for ca. 15 s at each potential to ensure steady-state currents (Figure 4). Although linear, Figure 4 gives a 70-mV not 59-mV slope. Higher than 59/n-mV slopes in analogous plots in rotated disk voltammetry¹³ of dissolved reactants at naked electrodes are ordinarily associated with slow charge transfer at the electrode-solution interface. In the present experiment, however, the larger slope is expected from the well-known (but little understood) broadening of cyclic voltammograms of electroactive polymer films,^{1e,2a,2o,15} which occurs also in the cyclic voltammetry of the Os and Ru polymers. The broadening has been attributed to a nonlinearity in the relationship between activity and coverage and has been semiempirically expressed as eq 3 by Albery and co-

(15) (a) Brown, A. P.; Anson, F. C. *Anal. Chem.* 1977, 49, 1589. (b) Smith, D. F.; Willman, K.; Kuo, K.; Murray, R. W. *J. Electroanal. Chem.* 1979, 95, 217.

Scheme II



Scheme III



workers.²⁰ An earlier treatment, with a different relation which was re-formulated by Ikeda¹⁶ for polymers, was made by Brown and Anson^{15a} for graphite electrode absorbates. Note that the Figure 4 data fit the Albery²⁰ formulation with $g = 0.84$ (—) somewhat better than does the Ikeda relation (eq 5 of ref 1e), with $G = -0.67$ (---).

Figures 3b and 3c show voltammograms where different constant values of E_{Au} were used while E_{Pt} was scanned. These are entirely understandable on the same basis as Figure 3a, where E_{Au} is 0 V vs. SSCE, the wave's $E_{1/2}$ occurs at $E_{\text{Pt}} \sim E^{\circ'} = 0.73$ V vs. SSCE, and the electron flow across the film is from Au to Pt. If $E_{\text{Au}} = E^{\circ'}$ (Figure 3b), the $E_{1/2}$ of the wave is still at $E_{\text{Pt}} = E^{\circ'}$, but current flows from Au to Pt or from Pt to Au depending upon whether E_{Pt} is more or less positive than E_{Au} . And if $E_{\text{Au}} = 0.9$ V vs. SSCE (Figure 3c), then nearly all of the polymer in contact with the gold is oxidized and electron flow from Pt to Au occurs only when E_{Pt} is less positive than E_{Au} . Finally, in Figure 3d, E_{Pt} is 0 V and E_{Au} is varied with a result analogous to Figure 3a, except that the Au charging current is large due to the large Au electrode area (Figure 2).

Following the reasoning used to obtain eq 1, we can obtain an equation that describes the redox conduction current at either electrode ($i_{\text{Pt}} = -i_{\text{Au}}$) in Figure 3a–d as a function of both E_{Pt} and E_{Au} :

$$(i_{\text{Pt}}/i_{\text{L}}) = \{1 + \exp[(gnF/RT)(E^{\circ'} - E_{\text{Pt}})]\}^{-1} - \{1 + \exp[(gnF/RT)(E^{\circ'} - E_{\text{Au}})]\}^{-1} \quad (4)$$

where i_{L} is given by eq 2. Overall, sandwich-electrode redox conduction voltammograms are well represented with simple equations based on electron diffusion.

Redox Conduction Currents for the Os(II/I) and Os(I/O) Couples in Poly[Os(bpy)₂(vpy)₂]ⁿ⁺ Films. By sweeping E_{Pt} to negative potentials relative to E_{Au} , the (formal) Os(I) and Os(0) oxidation states can be generated at the Pt surface and these states reoxidized at the Au electrode surface. Three situations result, depending on the Pt and Au potentials employed.

If E_{Au} is say 0 V and E_{Pt} is scanned past $E^{\circ'}$ for the Os(II/I) reaction (-1.32 V), the redox conduction is determined by D_{ct} for the Os(II/I) mixed-valent state (Scheme II). By scanning E_{Pt} more negatively, past $E^{\circ'} = -1.53$ V for the Os(I/O) reaction, the current will be determined by a combination of D_{ct} for the Os(II/I) and Os(I/O) mixed-valent states, with the concentration gradients for the two arranged (spatially) in series across the film. By the above notation, the electrode reactions and the comproportionation reaction occurring (presumably) within the film are shown in Scheme III. Schemes I–III are illustrated for a poly-[Os(bpy)₂(vpy)₂]ⁿ⁺ film in Figure 5, in which E_{Au} was maintained at 0 V vs. SSCE and E_{Pt} was scanned between +1.0 and -1.8 V. Three distinct current regions appear, around $E^{\circ'}$ for the three osmium reactions, at $E_1^{\circ'} = +0.72$ V for Os(III/II), at $E_2^{\circ'} = -1.32$ V for Os(II/I), and at $E_3^{\circ'} = -1.53$ V for Os(I/O). It is striking that the currents passed through the three mixed-valent states differ considerably; note that the current sensitivity for the left-hand side of Figure 5 is 50× greater than for the right-hand side. The limiting currents for the three current regions in Figure 5 were $i_{\text{L},1} = 39 \mu\text{A}$, $i_{\text{L},2} = 150 \mu\text{A}$, and $i_{\text{L},3} \sim 1900 \mu\text{A}$.

The third, important situation is when the Au electrode oxidizes Os(0) but not Os(I), i.e., $E_{\text{Au}} = -1.4$ V vs. SSCE, and E_{Pt} is scanned between more positive and more negative potentials than

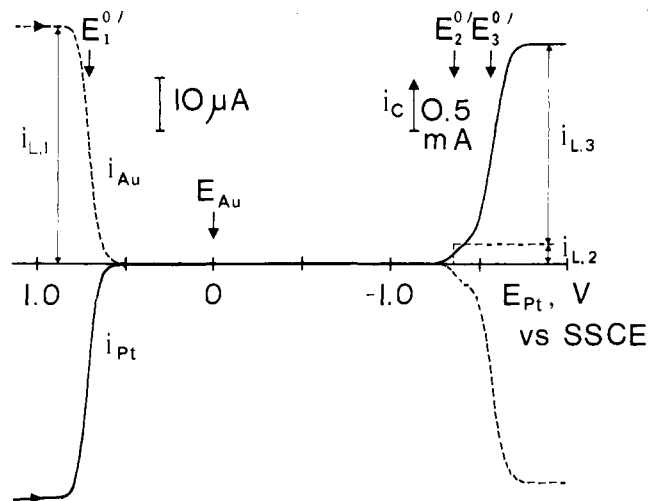


Figure 5. Four-electrode cyclic voltammetry at 10 mV/s of a 6.1×10^{-8} mol/cm² ($d = 365$ nm) Pt/poly[Os(bpy)₂(vpy)₂]²⁺/Au sandwich electrode with $E_{\text{Au}} = 0$ V vs. SSCE. Electrode surface area = 0.0032 cm², 0.1 M Et₄NClO₄/CH₃CN.

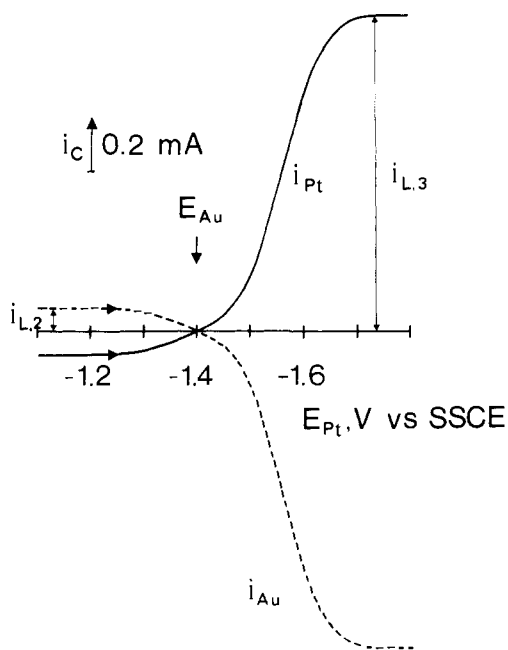
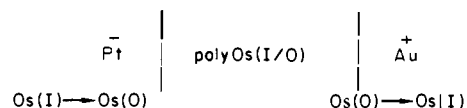


Figure 6. Four-electrode cyclic voltammetry at 10 mV/s of the sandwich electrode of Figure 5 (after some use and decrease in i_{L}) using $E_{\text{Au}} = -1.4$ V vs. SSCE: (—) i_{Pt} , (---) i_{Au} .

Scheme IV



this (Figure 6). In this case, the redox conduction currents when E_{Pt} is more positive occur by Scheme II (with Au and Pt reversed), and when E_{Pt} is more negative by the Os(I/O) mixed-valent state according to Scheme IV. The result in Figure 6 is for the same electrode as was used for Figure 5, but after some time of use and degradation,¹⁶ so that the limiting current for the Os(I/O) mixed-valent redox conduction is now lower ($i_{\text{L},3} = 1180 \mu\text{A}$), but remains obviously quite large as compared to the Os(III/II) currents recorded in Figure 5. The differences in limiting currents for the three Os mixed-valent states have been observed for many electrodes. For all three redox conduction waves, they are inversely

(16) The limiting current for the Os(1+/0) mixed-valent state slowly decays.

Table II. Electron Diffusion Coefficients, D_{ct} , for Reduced Mixed-Valent States in Poly[Os(bpy)₂(vpy)₂]²⁺ at 25 °C As Measured with Glass-Shrouded Sandwich Electrodes

$\Gamma_T \times 10^8$, mol/cm ²	$D_{ct} \times 10^9$, cm ² s ⁻¹		
	Os(III/II)	Os(II/I)	Os(I/0)
2.4	2.4		
3.9	5.8	9 ^a	100 ^a
4.6	8.6		150 ^a
5.6	3.6	17	130
5.6	7.0	33	290
6.0	13.0		280 ^a
6.1	4.8	24	160
6.8	6.8		140 ^a
7.6	10.0	21 ^a	170 ^a
8.9	6.6	35	290
9.5	8.4		
12.3	12.0	35 ^a	180 ^a
13.4	11.0	21 ^a	220 ^a
13.6	1.3		310 ^a
av D_{ct}	8 ± 3	24 ± 9	200 ± 70

^a Recalculated from low-temperature data; see text.

proportional to the film coverage (i.e., thickness) as predicted by eq 2, and give reasonably constant D_{ct} for each wave (Table II), based on $C_T = 1.5 \times 10^{-3}$ (see Experimental Section). The D_{ct} 's calculated for the Os(III/II) mixed-valent state from experiments using the Teflon and glass-shrouded electrodes, Tables I and II, 5×10^{-9} cm²/s and 8×10^{-9} cm²/s, respectively, are only slightly different.

Clearly, the effective electron mobilities in the poly[Os(bpy)₂(vpy)₂]²⁺ film are strongly dependent on the particular mixed-valent state generated and are especially large in the Os(I/0) state as seen from both Figures 5 and 6. The Os(I/0) state, in fact, can sustain very large currents; that in Figure 5 corresponds to a current density of 0.6 A/cm². Currents of this magnitude have not been heretofore reported in the polymer-coated electrode field. The possibility that the large currents might be driven by a voltage gradient in a film of intrinsically high conductivity Os(0) state were preliminarily explored. The entire film was placed in the Os(0) state, by making both E_{Pt} and E_{Au} electrodes more negative than $E^{o'}$ for the Os(I/0) reaction, and different in potential by 0.1 V. Some current flow was seen, but it was much smaller than the $i_{L,3}$ observed above, and so it seems that the large effective electron mobility depends principally on the presence of the Os(I/0) mixed-valent state and is a redox conduction current.

While redox conduction currents are driven by concentration gradients, and thus are fundamentally different from the normal concept of voltage gradient-driven conductivity, and furthermore must be referred to a reference electrode scale as is evident from Figure 3, observation of the large current passed by the Os(I/0) mixed-valent film makes comparison with currents passed by so-called "conducting organic polymers" of interest. We suggest that an operationally useful way to make such a comparison is to use the Δ_i/Δ_E slope of the redox conduction voltammogram at $E^{o'}$ of the polymer. This can be shown from the above relations to be

$$(d/A)(\Delta_i/\Delta_E)_{E=E^{o'}} = g(nF)^2 D_{ct} C_T / 4RT \quad (5)$$

For the Os(I/0) mixed-valent state, this corresponds to an apparent "conductivity" of $1.5 \times 10^{-4} \Omega^{-1} \text{cm}^{-1}$, which is at the low end of that of substituted polypyrrole organic conductors.¹⁷

Finally, we should note that the Os(II/I) and Os(I/0) D_{ct} values would have been difficult to obtain with other, transient method such as chronoamperometry, because of the proximity of the two voltammetric waves, and because D_{ct} and currents are large. Also, in the sandwich electrodes, Os(II/I) and Os(I/0) voltammetry (Figures 5 and 6) is much less stable (and less reproducible) than Os(III/II) sandwich-electrode voltammetry (Figure 3), but is at

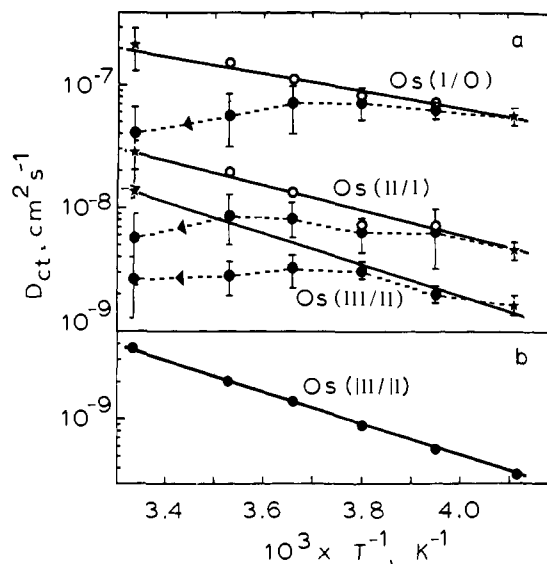


Figure 7. Arrhenius plots for temperature dependence of D_{ct} for [Os(bpy)₂(vpy)₂]²⁺ sandwich electrodes with Γ_T ranging from 5.6×10^{-8} to 14.5×10^{-8} mol/cm². ● represents measurements made proceeding from low to high temperature (showing effect of partial polymer decay); * represents measurements on virgin sandwich electrodes (non-decayed), O's are data points corrected for polymer decay (see text). Error bars are 2σ std long.

the same time more stable than our previous experience with similar polymer films in non-sandwich-electrode form has been.

Variable-Temperature Experiments. Limiting currents in sandwich electrodes have the activation barrier/temperature dependence expected of their electron self-exchange reaction origin. Os(III/II) redox conduction currents (Scheme I), for a given sandwich electrode, follow a stable Arrhenius temperature dependence from -35 to 25 °C (Figure 7b):

$$D_{ct} = D_0 \exp[-E_a/RT] \quad (6)$$

which gives a (typical) activation barrier $E_a = 5.8$ kcal/mol and (for the electrode shown, and assuming a constant $C_T = 1.5 \times 10^{-3}$ mol/cm³) $D_0 = 2.7 \times 10^{-4}$ cm²/s.

Redox conduction currents for the Os(II/I) and Os(I/0) voltammograms are also temperature dependent, but the sandwich electrodes were not sufficiently stable to obtain nondistorted Arrhenius plots, even when doing the measurements quickly starting from low temperatures (solid points, Figure 7a). The value of D_{ct} varies too much from electrode to electrode (Tables I and II) to allow solving of this problem by using a fresh electrode for measurement at each temperature. An approximation of the Os(II/I) and Os(I/0) barriers was obtained by noting that the instability-produced distortion (presumably caused by loss of redox conduction sites) also appeared in D_{ct} for the Os(III/II) wave, but only when potentials were swept through the Os(II/I) and Os(I/0) states (i.e., compare Os(III/II) in Figure 7a and Figure 7b). The assumption was then made that the fractional decay in Os(III/II), Os(II/I), and Os(I/0) currents was the same at each temperature, from which the latter, corrected currents (Figure 7a, open points) gave reasonably linear Arrhenius plots, the termini of which fall through more reliable points obtained by separate measurements on virgin sandwiches in the same multi-mini-electrode sample. This produced rough estimates for the Os(II/I) and Os(I/0) states, of $E_a = 4.5$ and 3.3 kcal/mol and $D_0 = 5.4 \times 10^{-5}$ and 4.5×10^{-5} cm²/s, respectively.

Origin of the Electron Mobilities. We have interpreted the currents flowing through the Os polymer films in terms of concentration gradient-driven redox conduction, which occurs by neighbor oxidized-reduced site electron exchange and is measured by the parameter D_{ct} . Microscopically, the value of D_{ct} in a given redox polymer is governed either by (i) the intrinsic barrier to electron self-exchange giving self-exchange rate k_{ex}^{pol} between redox sites, by (ii) the motions of the polymer lattice which control the

(17) Diaz, A. F.; Castillo, J.; Kanazawa, K. K.; Logan, J. A. *J. Electroanal. Chem.* **1982**, 133, 233.

collision rate between oxidized and reduced sites, or by (iii) the motions of the counterions whose presence is necessary to retain charge neutrality in the polymer.

Counterion diffusion (process iii) can be explicitly eliminated as a rate-controlling factor for the Os(III/II) electron diffusion, by a direct comparison of counterion vs. electron mobilities as was done previously¹⁸ for a related polymer film poly[Ru(vbpy)₃]²⁺. Rotated disk electrode currents for the poly[Os(bpy)₂(vpy)₂]³⁺ membrane-limited oxidation of Cl⁻ in 0.1 M Et₄NClO₄/CH₃CN give Cl⁻ permeability^{18c} of the polymer as $P D_{s,pol} = 3.5 (\pm 0.6) \times 10^{-7}$ cm²/s, independent of Γ_T and [Cl⁻]. This is 65× larger than the Os(III/II) electron mobility, and provided analogy is assumed between Cl⁻ and ClO₄⁻, shows that the electron self-exchange cannot be counterion mobility limited. The analogy between Cl⁻ and ClO₄⁻ is supported by remeasuring the Os(III/II) D_{ct} , in chloride medium (0.1 M Et₄NCl, based^{1e,21} on oxidation of [Os(bpy)₂Cl₂] at rotated poly[Os(bpy)₂(vpy)₂]²⁺ disks), finding that D_{ct} is essentially unchanged (4.8×10^{-9} cm²/s) from that in perchlorate medium (e.g., 5.4×10^{-9} cm²/s).

The increase in D_{ct} observed in the poly[Os(bpy)₂(vpy)₂]²⁺ film for Os(II/I) and Os(I/0) as compared to that for Os(III/II) reinforces the above conclusion; i.e., a D_{ct} which is counterion diffusion limited in the Os(III/II) state could show an increase upon change to a more reduced polymer state only if the counterion diffusion rate were enhanced by reducing the polymer. This seems unlikely given the magnitude of the change in counterion diffusion rate that would have to occur, and given that the reduced polymers have a diminished fixed ionic site capacity.

Consider next, for the Os(III/II) state, the distinction between intrinsic barrier (process i) and polymer lattice mobility (process ii) control of D_{ct} . The distinction is made by converting D_{ct} into an apparent electron self-exchange rate k_{ex}^{app} , for comparison to the barrier-controlled self-exchange rate k_{ex}^{homo} known¹⁹ for [Os(bpy)₃]^{3+/2+} in homogeneous solution. Converting D_{ct} to k_{ex}^{app} is straightforward if one assumes that the collision rate via polymer lattice mobility (process ii) is controlling, using the Smoluchowski equation²⁰ for a collision rate-controlled reaction

$$k_{ex}^{app} = 4 \times 10^{-3} \pi N (4r D_{ct}) \quad (7)$$

where for the Os polymer the collision radius, r , is taken as 0.7 nm, and D_{ox} and D_{red} are taken as equal since the electron and hole motions are correlated. Note that assuming rate control by process ii is equivalent to stating that $k_{ex}^{pol} \gg k_{ex}^{app}$.

Converting D_{ct} to k_{ex}^{app} is less obvious for control by process i (i.e., $k_{ex}^{pol} \sim k_{ex}^{app}$), but the following line of reasoning suggests that eq 7 allows a conceptually valid approximation of k_{ex}^{app} even in this case. Consider that, in a barrier-controlled homogeneous solution reaction, the reactant diffusion rate is relatively fast, and so many collisions occur which are not fruitful in producing electron transfer. In this case, k_{ex}^{app} calculated from eq 7 (using the true reactant diffusion coefficient) would clearly be too large. Consider, on the other hand, knowing in the solution (somehow) the rate of reactant diffusion which would lead *only* to electron-transfer-producing collisions; this (smaller) diffusion coefficient used in eq 7 would yield a k_{ex}^{app} more closely approximating the barrier-controlled k_{ex}^{homo} . Such a measure of solely *fruitful* collisions is not easily made (as a diffusion coefficient) in homogeneous solution, but in the electron transport problem in fixed site redox polymers, this is, in fact, the diffusion coefficient that is measured. That is, D_{ct} measures inherently only the electron-transfer fruitful collision rate; excess, non-electron-transferring collisions do not produce a current flow.

Using $D_{ct} = 5 \times 10^{-9}$ cm²/s in eq 7, we then calculate $k_{ex}^{app} = 1 \times 10^7$ M⁻¹ s⁻¹ for Os(III/II). This value is close to the homogeneous rate,¹⁹ 2.2×10^7 M⁻¹ s⁻¹, i.e., $k_{ex}^{app} \sim k_{ex}^{homo}$. From the

above reasoning, that eq 7 is exact if process ii controls, and gives an approximation of k_{ex}^{app} if process i controls, the observation that $k_{ex}^{app} \sim k_{ex}^{homo}$ strongly implies that D_{ct} for the Os(III/II) state is barrier controlled (process i). We have recently shown²¹ through successful Marcus theory correlation, not involving D_{ct} considerations, that the electron self-exchange rate for at least the outermost monomolecular layer of sites in a poly[Os(bpy)₂(vpy)₂]²⁺ film is close to the homogeneous rate; i.e., for those sites apparently $k_{ex}^{pol} \sim k_{ex}^{homo}$. This result is consistent with the eq 7 based comparison if $k_{ex}^{pol} \sim k_{ex}^{homo}$ for the interior as well as the polymer/solution interface Os sites, which seems reasonable.

[For the Ru(III/II) state in poly[Ru(vbpy)₃]²⁺, current (and we believe freer from polymer degradation effects) evaluations of D_{ct} (1.9×10^{-9} , 1.0×10^{-9} , and 6.2×10^{-10} cm²/s, calculated from $D_{ct}^{1/2} C_T = 5.6$, 5.1 , and 4.0×10^{-8} , respectively, in Table I) are larger than the older, chronoamperometry result^{1d} (1.9×10^{-10} cm²/s) which suggested to us polymer lattice motion control of D_{ct} . Application of eq 7 to these values gives $k_{ex}^{app} = 4 \times 10^6$, 2×10^6 , and 1.3×10^6 M⁻¹ s⁻¹, respectively, which are not too different from the $k_{ex}^{homo} = 8.3 \times 10^6$ M⁻¹ s⁻¹ known for¹⁸ [Ru(bpy)₃]^{3+/2+}. This comparison suggests that D_{ct} in this polymer may, like the present Os polymer, be best interpreted in terms of control by process i.]

With respect to D_{ct} for the reduced osmium polymer states Os(II/I) and Os(I/0), we will not try to discern which of the three processes controls electron mobility. The above discussion indicates, however, that the D_{ct} data reflect at least the lower limits for self-exchange rates k_{ex}^{pol} between Os(II/I) and Os(I/0) sites. Using eq 7 and average D_{ct} data in Table II gives $k_{ex}^{app} \sim 5 \times 10^7$ and 4×10^8 M⁻¹ s⁻¹, respectively, and accordingly the electron self-exchange rate constants k_{ex}^{app} for Os(III/II), Os(II/I), and Os(I/0) are in the proportion 1 : >3 : >25 in the poly[Os(bpy)₂(vpy)₂]²⁺ polymer film.

Homogeneous k_{ex}^{homo} values do not, except as estimations,²² exist for comparison to the apparent Os(II/I) and Os(I/0) self-exchange rates. Heterogeneous electron-transfer rate constants for [Os(bpy)₃]²⁺ at Hg electrodes in DMF solvent have been reported,²³ however, and their relative values surprisingly fall in a different order from that observed in the polymer, namely, 1 : 0.2 : 0.3 for the Os(III/II), Os(II/I), and Os(I/0) electrode reactions. The reported rationale²³ for the Os(II/I) rate being slower than that for Os(III/II) was that the Os(III/II) reaction involves loss or gain of an electron in a primarily metal-centered orbital, whereas the Os(II/I) reaction involves a change in electronic configuration by placing the added electron in a ligand centered orbital. If the same argument were applied to the polymer k_{ex}^{pol} data, one would conclude that such a change in electronic configuration does not occur in making poly[Os(bpy)₂(vpy)₂]¹⁺ and poly[Os(bpy)₂(vpy)₂]⁰ states, i.e., that in producing these states the electrons enter orbitals that are more metal centered than would be the case in solutions of the monomers of these complexes. That this indeed may be the case is given precedent in a recent report by DeArmond et al.²⁴ that precipitation of doubly reduced Ru and Fe polypyridine complexes from acetonitrile solution is accompanied in the precipitate by electronic isomerization from a ligand localized configuration to a more metal- than ligand-centered one. This rationale for the observed polymer k_{ex}^{pol} ordering is at this point clearly speculative, and should bear further scrutiny.

Redox Conduction Currents across a Bilayer, Pt/poly[Ru(bpy)₂(vpy)₂]²⁺/poly[Os(bpy)₂(vpy)₂]²⁺/Au. When a redox polymer film is separated from an electrode by a different redox polymer, then oxidation or reduction of the outer polymer by the electrode must be mediated by redox conduction through the inner polymer.⁶ For example, a poly[Os(bpy)₂(vpy)₂]²⁺ film ($E^{\circ'} = 0.73$ V) separated from the electrode by a poly[Ru(bpy)₂(vpy)₂]²⁺ film ($E^{\circ'} = 1.22$ V) is not oxidized at an electrode potential of 0.73 V, because at this potential the ruthenium polymer is in its

(18) (a) Ikeda, T.; Schmehl, R.; Denisevich, P.; Willman, K.; Murray, R. W. *J. Am. Chem. Soc.* **1982**, *104*, 2683. (b) Facci, J. S. University of North Carolina, unpublished results, 1982. (c) P and $D_{s,pol}$ represent the partition and diffusion coefficients of Cl⁻ in the polymer, respectively.

(19) Chan, M. S.; Wahl, A. C. *J. Phys. Chem.* **1978**, *82*, 2543.

(20) Kahlweit, M. In "Physical Chemistry An Advanced Treatise", Eyring, H., Ed., Academic Press: New York, 1975; Vol. VII, pp 507, 677.

(21) Leidner, C. R.; Murray, R. W. *J. Am. Chem. Soc.* **1984**, *106*, 1606.

(22) Sutin, N.; Creutz, C. *Pure Appl. Chem.* **1980**, 2717.

(23) Saji, T.; Aoyagui, S. *J. Electroanal. Chem.* **1975**, *63*, 31.

(24) Morris, D. E.; Hanck, K. W.; DeArmond, M. K. *J. Am. Chem. Soc.* **1983**, *105*, 3032.

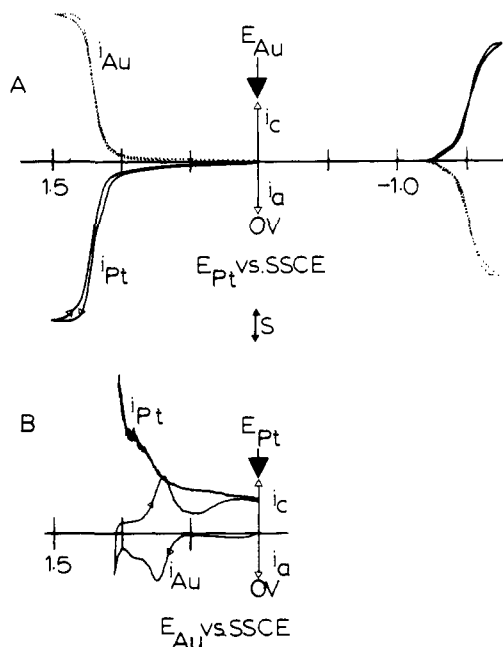


Figure 8. Four-electrode cyclic voltammetry of a bilayer sandwich electrode Pt/poly[Ru(bpy)₂(vpy)₂]²⁺/poly[Os(bpy)₂(vpy)₂]²⁺/Au with $\Gamma_{\text{Ru}} = 1.0 \times 10^{-8}$ and $\Gamma_{\text{Os}} = 9.4 \times 10^{-8}$ mol/cm². Curve A: $E_{\text{Au}} = 0$ V vs. SSCE and E_{Pt} scanned at 20 mV/s, $S = 5$ and 250 μA for positive and negative E_{Pt} , respectively. Curve B: $E_{\text{Pt}} = 0$ V vs. SSCE and E_{Au} scanned at 20 mV/s, $S = 5.0$ μA for i_{Au} and 0.25 μA for i_{Pt} , 0.1 M Et₄NClO₄/CH₃CN.

Ru(II) state, not a mixed-valent state and so is an insulator. At potentials near 1.22 V the ruthenium polymer conducts and so the osmium polymer is oxidized.

We have prepared a bilayer electrode sandwich of these two polymers to illustrate the rectifying behavior of the polymer

film/film junction, with results shown in Figure 8. For $E_{\text{Au}} = 0$ V vs. SSCE, the redox conduction waves have a similar appearance to those obtained for a sandwich using a film of a single polymer. The redox conductions due to the M(II/I) and M(II/0) mixed-valent states (Schemes II and III) occur with similar magnitude ($i_L = 700$ μA) as observed for osmium, and at the same potentials as for nonsandwich films of osmium or ruthenium polymer alone, since $E^{\circ'}$ for the M(II/I) and M(I/0) reactions are approximately the same for both polymers. The redox conduction due to the M(III/II) reaction occurs with similar i_L (23 μA) to that with just one polymer, and it is centered on $E^{\circ'} = 1.22$ V vs. SSCE for the ruthenium polymer. Redox conduction is not observed at E_{Pt} near the osmium polymer $E^{\circ'}$. The latter is the expected result⁶ since the bilayer cannot conduct electrons until both polymer films are mixed valent, which requires that E_{Pt} be close to $E^{\circ'}$ for the ruthenium polymer. A quantitative treatment of i_L for the bilayer is given elsewhere.²⁵

The corollary result is obtained if E_{Pt} is kept constant at 0 V vs. SSCE and E_{Au} is varied. As shown in Figure 8B, a non-steady-state wave for oxidation and reduction of the osmium part of the film is observed at the Au electrode, centered at $E^{\circ'}$ for the osmium polymer. No significant current is seen at the Pt electrode, which has a potential sufficient to re-reduce the Os(III) generated by the Au electrode. This is, of course, because the inner ruthenium polymer film remains as Ru(II) and is an insulator in this non-mixed-valent state.

Acknowledgment. This research was supported in part by the Office of Naval Research and by grants from the National Science Foundation and from the Chevron Research Company.

Registry No. Poly[Ru(bpy)₂(vpy)₂]²⁺, 88670-65-9; poly[Ru(vbpy)₃]²⁺, 81206-05-5; poly[Os(bpy)₂(vpy)₂]²⁺, 88728-97-6.

(25) Pickup, P. G.; Leidner, C. R.; Denisevich, P.; Murray, R. W., *J. Electroanal. Chem.*, in press.

Water-Soluble α,ω -Bis(paraquat) Amphiphiles Form Monolayer Membrane Vesicles, Micelles, and Crystals by Stepwise Anion Exchange or Photochemical Reduction

Jürgen-Hinrich Fuhrhop,* Detlev Fritsch, Bernd Tesche, and Hardi Schmiady

Contribution from the Institut für Organische Chemie der Freien Universität Berlin, 1000 Berlin 33, West Germany, and Fritz-Haber-Institut der Max-Planck-Gesellschaft, Abt. Elektronenmikroskopie, 1000 Berlin 33, West Germany. Received July 13, 1983

Abstract: 1,1'-[(1,8-Dioxo-1,8-octanediy)bis(oxy-11,1-undecanediy)]bis[1'-methyl-4,4'-bipyridinium] tetrachloride (**3a**), 1,1'-[(1,12-dioxo-1,12-dodecanediy)bis(oxy-11,1-undecanediy)]bis[1'-methyl-4,4'-bipyridinium] tetrachloride (**3b**), the corresponding dibromide diiodide (**3f**), 1,1'-[(1,18-dioxo-1,18-octadecanediy)bis(oxy-11,1-undecanediy)]bis[1'-methyl-4,4'-bipyridinium] tetrachloride (**3c**), the corresponding tetra-perchlorate (**3d**), and trichloride monoperochlorate (**3e**) have been prepared. The solubility and the aggregation behavior of these compounds largely depend on the nature of the inorganic anions. The tetrachlorides **3a–c** are readily soluble in water. Titration of **3c** with 1 equiv of sodium perchlorate or irradiation of **3c** with visible light in the presence of ferrocyanide lead to vesiculation. Vesicles were also obtained by dissolving the dibromide diiodide **3f** in water. A turbid emulsion of the tetra-perchlorate **3d** clears on heating to 70 °C. After cooling to room temperature vesicles were formed; after 24 h at room temperature crystals of a thickness ≤ 100 Å were observed in electron micrographs. This corresponds to a crystalline monolayer. The electron micrographs also show micelles of diameters ~ 100 Å.

Our general investigation of monolayer vesicle membranes has shown that α,ω -bifunctional amphiphiles produce unsymmetric vesicles if the size of both head groups is different.¹ Curvature is produced by orientation of the large head groups to the outside

and the small head groups to the inside. An early report by our group that symmetric α,ω -bis(bipyridinium) amphiphile **1** gives vesicles² was partly in error. Vesicle formation rather depended

* Address correspondence to this author at the Freien Universität.

(1) Fuhrhop, J.-H.; Mathieu, J. *J. Chem. Soc., Chem. Commun.* 1983, 144. See also: Okahata, Y.; Kunitake, T. *J. Am. Chem. Soc.* 1979, 101, 5231.